

# Quark Wigner Distributions and Orbital Angular Momentum in Light-front Dressed Quark Model

Asmita Mukherjee, Sreeraj Nair and Vikash Kumar Ojha

*Department of Physics,  
Indian Institute of Technology Bombay,  
Powai, Mumbai 400076, India.*

(Dated: December 3, 2024)

## Abstract

We calculate the Wigner functions for a quark target dressed with a gluon. These give a combined position and momentum space information of the quark distributions and are related to both generalized parton distributions (GPDs) and transverse momentum dependent parton distributions (TMDs). We calculate and compare the different definitions of quark orbital angular momentum in this model. We compare our results with other model calculations.

## I. INTRODUCTION

In classical physics, a system of particles can be described in terms of phase space distributions, which represent the density of particles at a point in the phase space at a given time. In quantum mechanics, position and momentum operators do not commute and they cannot be determined simultaneously. Thus in quantum mechanics one cannot define phase space distributions. Wigner distributions in quantum mechanics have been introduced long ago [1], which can be thought of as quantum mechanical phase space distributions, however it cannot be interpreted as probability distribution for the reason above and is not positive definite. Wigner distributions become classical phase space distributions in the limit  $\hbar \rightarrow 0$ . A quantum mechanical Wigner distribution for the quarks and gluons in the rest frame of the nucleon was introduced in [2, 3]. Reduced Wigner functions are obtained from the seven dimensional most general Wigner distributions by integrating the minus component of the momentum. Reduced Wigner distributions are functions of three position and three momentum variables and as discussed above are not measurable. To obtain measurable quantities one has to integrate over more variables. Integrating out the momentum variables one can relate the reduced Wigner distributions to generalized parton distributions (GPDs) and integrating out the position variables one gets the transverse momentum dependent parton distributions (TMDs). Thus the Wigner distributions can be thought of as more general mother distributions in which both position and momentum space information of quarks and gluons are encoded.

Wigner distributions are related to the generalized transverse momentum dependent correlation functions (GPCFs) [4] of the nucleon, which are the fully unintegrated, off-diagonal quark-quark correlators. If one integrates over the minus component of the momentum (light-cone energy) one gets the generalized transverse momentum dependent parton distributions (GTMDs). These are functions of the 3-momentum of the quark and the momentum transfer to the nucleon  $\Delta_\mu$ . In [5] the authors introduced five dimensional Wigner distributions in infinite momentum frame by integrating the GTMDs over the momentum transfer in the transverse direction  $\Delta_\perp$ . These Wigner distributions are functions of the two position and three momentum variables. Working in infinite momentum frame, or equivalently using the light-cone formalism has several advantages as the transverse boosts are Galilean, or do not

involve dynamics, and longitudinal boost is just a scale transformation [6]. So it is easier to have an intuitive picture of the parton distributions in the nucleon which is boost invariant. As discussed before, Wigner distributions do not have probabilistic interpretation due to uncertainty principle. Integrating out one or more variables one can define new distributions that have probabilistic interpretation. Depending on whether the nucleon and the quark is polarized or unpolarized several such distributions can be defined. In this work we shall restrict ourselves to longitudinal polarization's only. As Wigner distributions cannot be measured, model calculations are of importance to understand what kind of information about the quark-gluon correlation in the nucleon can be obtained from them as well as to verify to what extent various model dependent and model independent relations among various distributions are satisfied. However, integrating out more variables gives measurable quantities having the interpretation of probability densities. In [5] the Wigner distributions for quarks and gluons have been studied in light cone constituent quark model and in light-cone chiral quark soliton model. Both these models have no gluonic degrees of freedom and the Wilson line becomes unity.

Quark orbital angular momentum (OAM) contribution to the total spin of the nucleon has gained considerable attention since the EMC experiments [7] which showed that the quark intrinsic spin contribution was less than expected. Also recent polarized beam experiments suggest that the gluon polarization contribution to the total spin of the proton is very small which makes the OAM contribution even more important. Wigner distributions are related to the OAM carried by the quarks in the nucleon. As is well known, a substantial part of the spin of the nucleon comes from quark and gluon OAM. The issue of gauge invariance and experimental measurability of the OAM contribution complicates the issue of a full understanding of such contributions [8]. Theoretically there exist mainly two definitions of OAM : one obtained from the sum rules of GPDs and the other, canonical OAM distribution in the light cone gauge. It has been shown in the literature that these two different distributions are projections of Wigner distributions with different choice of gauge links and they are related by a gauge dependent potential term. In [5] the canonical OAM in light-front gauge is shown to be related to the twist three GPDs. In this work we calculate the OAM using the Wigner distributions in light cone gauge and setting the gauge link to unity for a dressed quark; we also relate it to a previous calculation of canonical OAM in the same gauge.

## II. WIGNER DISTRIBUTIONS

The Wigner distribution of quarks can be defined as the two-dimensional Fourier transforms of the generalized transverse momentum distributions (GTMDs) [4, 5]

$$\rho^{[\Gamma]}(\vec{b}_\perp, \vec{k}_\perp, x, \vec{\sigma}) = \int \frac{d^2\Delta_\perp}{(2\pi)^2} e^{-i\Delta_\perp \cdot \vec{b}_\perp} W^{[\Gamma]}(\Delta_\perp, \vec{k}_\perp, x, \vec{\sigma}); \quad (1)$$

where  $\Delta_\perp$  is momentum transfer of nucleon in transverse direction and  $\vec{b}_\perp$  is 2 dimensional vector in impact parameter space conjugate to  $\Delta_\perp$ .  $W^{[\Gamma]}$  is the quark-quark correlator given by

$$\begin{aligned} W^{[\Gamma]}(\vec{\Delta}_\perp, \vec{k}_\perp, x, \vec{\sigma}) &= \left\langle p^+, \frac{\Delta_\perp}{2}, \vec{\sigma} \left| W^{[\Gamma]}(0_\perp, k_\perp, x) \right| p^+, -\frac{\Delta_\perp}{2}, \vec{\sigma} \right\rangle \\ &= \frac{1}{2} \int \frac{dz^- d^2 z_\perp}{(2\pi)^3} e^{i(xp^+ z^- / 2 - k_\perp \cdot z_\perp)} \left\langle p^+, \frac{\Delta_\perp}{2}, \vec{\sigma} \left| \bar{\psi}(-\frac{z}{2}) \Omega \Gamma \psi(\frac{z}{2}) \right| p^+, -\frac{\Delta_\perp}{2}, \vec{\sigma} \right\rangle \Big|_{z^+=0}. \end{aligned} \quad (2)$$

We define the initial and final dressed quark state in the symmetric frame[9] where  $p^+$  and  $\sigma$  defines the average longitudinal momentum of the target state and its polarization respectively.  $x = k^+/p^+$  is fraction of average longitudinal momentum of nucleon carried by the quark. In the symmetric frame the transverse momentum transfer( $\Delta_\perp$ ) has the  $\Delta_\perp \rightarrow -\Delta_\perp$  symmetry.  $\Omega$  is the gauge link needed for color gauge invariance. In this work, we use the light-front gauge and take the gauge link to be unity. The symbol  $\Gamma$  represents the Dirac matrix defining the types of quark densities.

In this work, we calculate the above Wigner distributions in a quark state dressed with a gluon. The state can be expanded in Fock space in terms of multi-parton light-front wave functions (LFWFs) [10]

$$\begin{aligned} |p^+, p_\perp, \sigma\rangle &= \Phi^\sigma(p) b_\sigma^\dagger(p) |0\rangle + \sum_{\sigma_1 \sigma_2} \int [dp_1] \int [dp_2] \sqrt{16\pi^3 p^+} \delta^3(p - p_1 - p_2) \\ &\quad \Phi_{\sigma_1 \sigma_2}^\sigma(p; p_1, p_2) b_{\sigma_1}^\dagger(p_1) a_{\sigma_2}^\dagger(p_2) |0\rangle; \end{aligned} \quad (3)$$

where  $[dp] = \frac{dp^+ d^2 p_\perp}{\sqrt{16\pi^3 p^+}}$  and  $\Phi_{\sigma_1 \sigma_2}^\sigma$  is the two particle (quark-gluon) light-front wave function (LFWF).  $\sigma_1$  and  $\sigma_2$  are the helicities of the quark and gluon respectively. The two particle



LFWF is related to the boost invariant LFWF;  $\Psi_2(x, q_\perp) = \Phi_2\sqrt{P^+}$ . These can be calculated perturbatively as [10]:

$$\Psi_{\sigma_1\sigma_2}^\sigma(x, q_\perp) = \frac{1}{\left[m^2 - \frac{m^2+(q_\perp)^2}{x} - \frac{(q_\perp)^2}{1-x}\right]} \frac{g}{\sqrt{2(2\pi)^3}} T^a \chi_{\sigma_1}^\dagger \frac{1}{\sqrt{1-x}} \left[ -2\frac{q_\perp}{1-x} - \frac{(\sigma_\perp \cdot q_\perp)\sigma_\perp}{x} + \frac{im\sigma_\perp(1-x)}{x} \right] \chi_{\sigma}(\epsilon_{\perp\sigma_2})^*. \quad (4)$$

We use the two component formalism [11];  $\chi$  is the two component spinor,  $m$  is the mass of the quark. In this work we investigate the Wigner distributions for unpolarized and longitudinally polarized nucleons and the relevant correlators are with  $\Gamma = \gamma^+$  and  $\gamma^+\gamma_5$ . The single particle sector contributes through the normalization of the state, which is important to get the complete contribution at  $x = 1$ . In this work we calculate the contribution to the quark-quark correlator and the Wigner distribution from the two particle sector in the Fock space expansion. This is given by

$$W^{[\gamma^+]}(\Delta_\perp, k_\perp, x, \sigma) = \frac{1}{(2\pi)^3} \sum_{\sigma_1, \sigma_2} \Psi_{\sigma_1\sigma_2}^{*\sigma}(x, q'_\perp) \Psi_{\sigma_1\sigma_2}^\sigma(x, q_\perp), \quad (5)$$

$$W^{[\gamma^+\gamma_5]}(\Delta_\perp, k_\perp, x, \sigma) = \frac{1}{(2\pi)^3} \sum_{\sigma_1, \sigma_2, \lambda_1} \Psi_{\lambda_1\sigma_2}^{*\sigma}(x, q'_\perp) \chi_{\lambda_1}^\dagger \sigma_3 \chi_{\sigma_1} \Psi_{\sigma_1\sigma_2}^\sigma(x, q_\perp); \quad (6)$$

where the Jacobi relation for the transverse momenta in the symmetric frame is given by  $q'_\perp = k_\perp - \frac{\Delta_\perp}{2}(1-x)$  and  $q_\perp = k_\perp + \frac{\Delta_\perp}{2}(1-x)$ . In this work we only consider the case of the target state (dressed quark) with longitudinal polarization. We use the symbol  $\rho_{\lambda\lambda'}$  for Wigner distributions, where  $\lambda(\lambda')$  is longitudinal polarization of nucleon(quark). These four Wigner distributions have been defined in [5] as

$$\rho_{UU}(\vec{b}_\perp, \vec{k}_\perp, x) = \frac{1}{2} \left[ \rho^{[\gamma^+]}(\vec{b}_\perp, \vec{k}_\perp, x, +\vec{e}_z) + \rho^{[\gamma^+]}(\vec{b}_\perp, \vec{k}_\perp, x, -\vec{e}_z) \right] \quad (7)$$

is the Wigner distribution of unpolarized quarks in unpolarized target state.

$$\rho_{LU}(\vec{b}_\perp, \vec{k}_\perp, x) = \frac{1}{2} \left[ \rho^{[\gamma^+]}(\vec{b}_\perp, \vec{k}_\perp, x, +\vec{e}_z) - \rho^{[\gamma^+]}(\vec{b}_\perp, \vec{k}_\perp, x, -\vec{e}_z) \right] \quad (8)$$

is the distortion due to longitudinal polarization of the target state.

$$\rho_{UL}(\vec{b}_\perp, \vec{k}_\perp, x) = \frac{1}{2} \left[ \rho^{[\gamma^+ \gamma_5]}(\vec{b}_\perp, \vec{k}_\perp, x, +\vec{e}_z) + \rho^{[\gamma^+ \gamma_5]}(\vec{b}_\perp, \vec{k}_\perp, x, -\vec{e}_z) \right] \quad (9)$$

represents distortion due to the longitudinal polarization of quarks, and

$$\rho_{LL}(\vec{b}_\perp, \vec{k}_\perp, x) = \frac{1}{2} \left[ \rho^{[\gamma^+ \gamma_5]}(\vec{b}_\perp, \vec{k}_\perp, x, +\vec{e}_z) - \rho^{[\gamma^+ \gamma_5]}(\vec{b}_\perp, \vec{k}_\perp, x, -\vec{e}_z) \right] \quad (10)$$

represents the distortion due to the correlation between the longitudinal polarized target state and quarks.

In our case,  $+\vec{e}_z$  and  $-\vec{e}_z$  correspond to helicity up and down of the target state, respectively.

In the model we consider,  $\rho_{LU} = \rho_{UL}$  and the final expression for the three independent Wigner distribution are as follows:

$$\rho_{UU}^{[\gamma^+]}(b_\perp, k_\perp, x) = \int d\Delta_x \int d\Delta_y \frac{\cos(\Delta_\perp \cdot b_\perp)}{D(q_\perp)D(q'_\perp)} \left[ I_1 + \frac{4m^2(1-x)}{x^2} \right]; \quad (11)$$

$$\rho_{LU}^{[\gamma^+]}(b_\perp, k_\perp, x) = \int d\Delta_x \int d\Delta_y \frac{\sin(\Delta_\perp \cdot b_\perp)}{D(q_\perp)D(q'_\perp)} \left[ 4(k_x \Delta_y - k_y \Delta_x) \frac{(1+x)}{x^2(1-x)} \right]; \quad (12)$$

$$\rho_{LL}^{[\gamma^+ \gamma_5]}(b_\perp, k_\perp, x) = \int d\Delta_x \int d\Delta_y \frac{\cos(\Delta_\perp \cdot b_\perp)}{D(q_\perp)D(q'_\perp)} \left[ I_1 - \frac{4m^2(1-x)}{x^2} \right]; \quad (13)$$

where  $A_x, A_y$  are  $x, y$  component of  $A_\perp$  and

$$D(k_\perp) = \left( m^2 - \frac{m^2 + (k_\perp)^2}{x} - \frac{(k_\perp)^2}{1-x} \right) \quad I_1 = 4 \left( (k_\perp)^2 - \frac{\Delta_\perp^2(1-x)^2}{4} \right) \frac{(1+x^2)}{x^2(1-x)^3}.$$

In all of the equations above we have taken the real part of the Fourier transform in Eq.(1).

### III. ORBITAL ANGULAR MOMENTUM OF QUARKS

In [4] it has been shown that the quark-quark correlator in Eq.(2) defining the Wigner distributions can be parameterized in terms of generalized transverse momentum dependent parton distributions (GTMDs). For the twist two case we have four GTMDs ( $F_{1,i}$ ) corresponding to  $\gamma^+$  and four more for  $\gamma^+ \gamma_5$  ( $G_{1,i}$ )

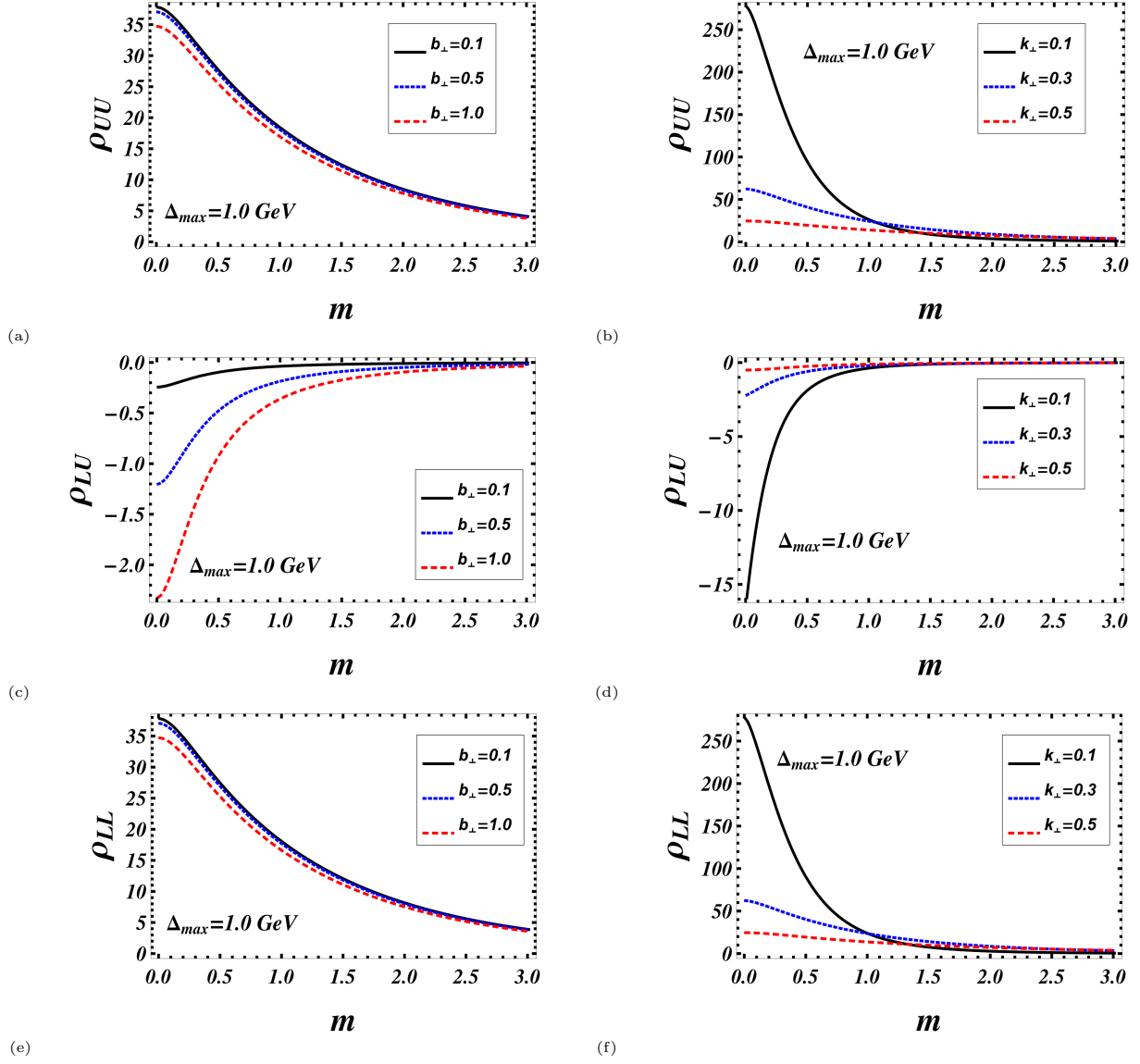


FIG. 1: (Color online) Plots of the Wigner distributions vs  $m$  (mass in GeV) for fixed values of  $b_{\perp}$  and  $k_{\perp}$  at  $\Delta_{max} = 1.0$  GeV. All the plots on the left (a,c,e) are for three fixed values of  $b_{\perp}$  (0.1,0.5,1.0) in  $\text{GeV}^{-1}$  where  $k_{\perp} = 0.4$  GeV. Plots on the right (b,d,f) are for three fixed values of  $k_{\perp}$  (0.1,0.3,0.5) in  $\text{GeV}$  where and  $b_{\perp} = 0.4$   $\text{GeV}^{-1}$ . For all plots we took  $\vec{k}_{\perp} = k_{\perp} \hat{j}$  and  $\vec{b}_{\perp} = b_{\perp} \hat{j}$ .

$$W_{\lambda,\lambda'}^{[\gamma^+]} = \frac{1}{2M} \bar{u}(p', \lambda') \left[ F_{1,1} - \frac{i\sigma^{i+} k_{i\perp}}{P^+} F_{1,2} - \frac{i\sigma^{i+} \Delta_{i\perp}}{P^+} F_{1,3} + \frac{i\sigma^{ij} k_{i\perp} \Delta_{j\perp}}{M^2} F_{1,4} \right] u(p, \lambda); \quad (14)$$

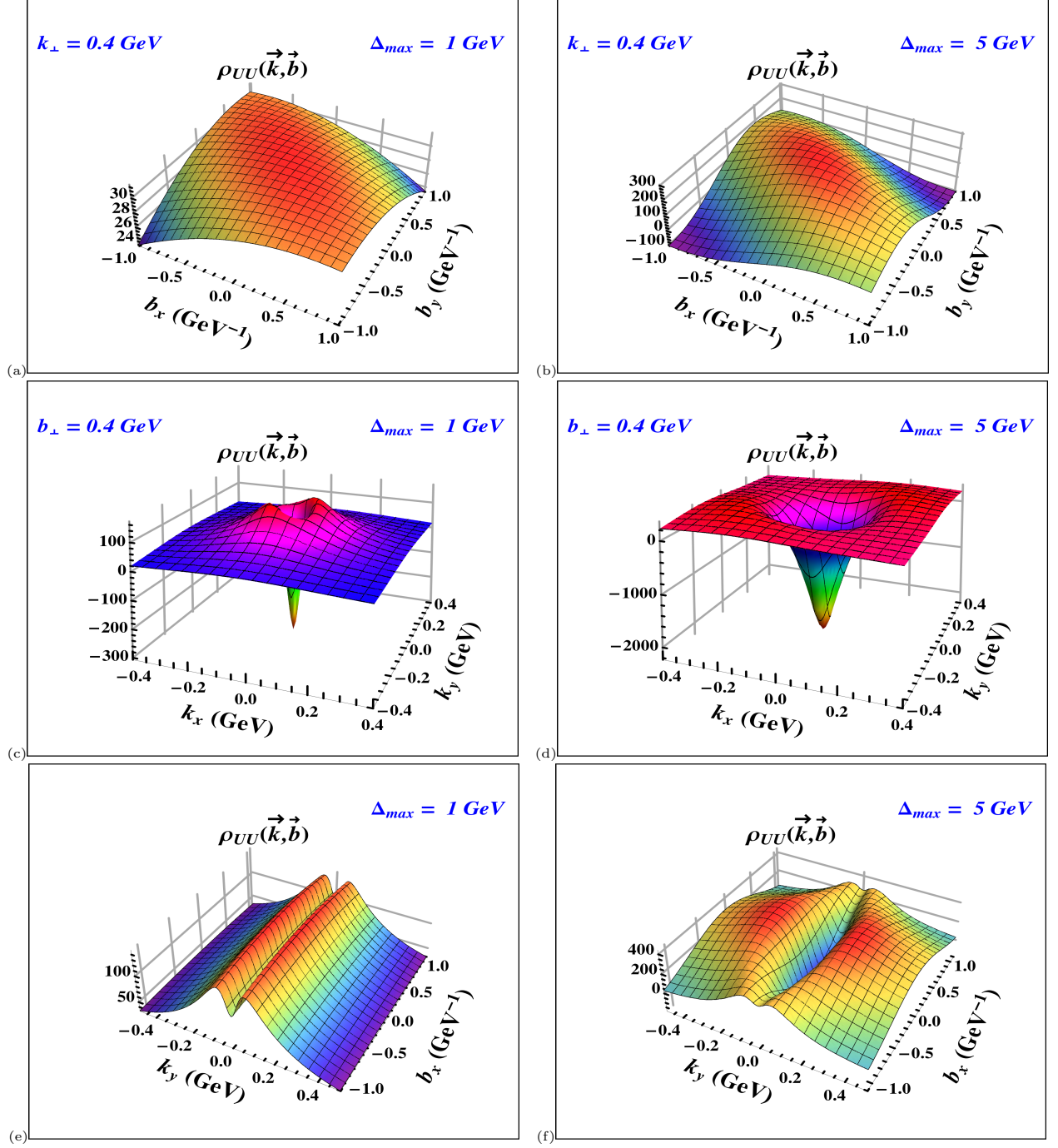


FIG. 2: (Color online) 3D plots of the Wigner distributions  $\rho_{UU}$ . Plots (a) and (b) are in  $b$  space with  $k_{\perp} = 0.4 \text{ GeV}$ . Plots (c) and (d) are in  $k$  space with  $b_{\perp} = 0.4 \text{ GeV}^{-1}$ . Plots (e) and (f) are in mixed space where  $k_x$  and  $b_y$  are integrated. All the plots on the left panel (a,c,e) are for  $\Delta_{max} = 1.0 \text{ GeV}$ . Plots on the right panel (b,d,f) are for  $\Delta_{max} = 5.0 \text{ GeV}$ . For all the plots we kept  $m = 0.33 \text{ GeV}$ , integrated out the  $x$  variable and we took  $\vec{k}_{\perp} = k_{\hat{j}}$  and  $\vec{b}_{\perp} = b_{\hat{j}}$ .

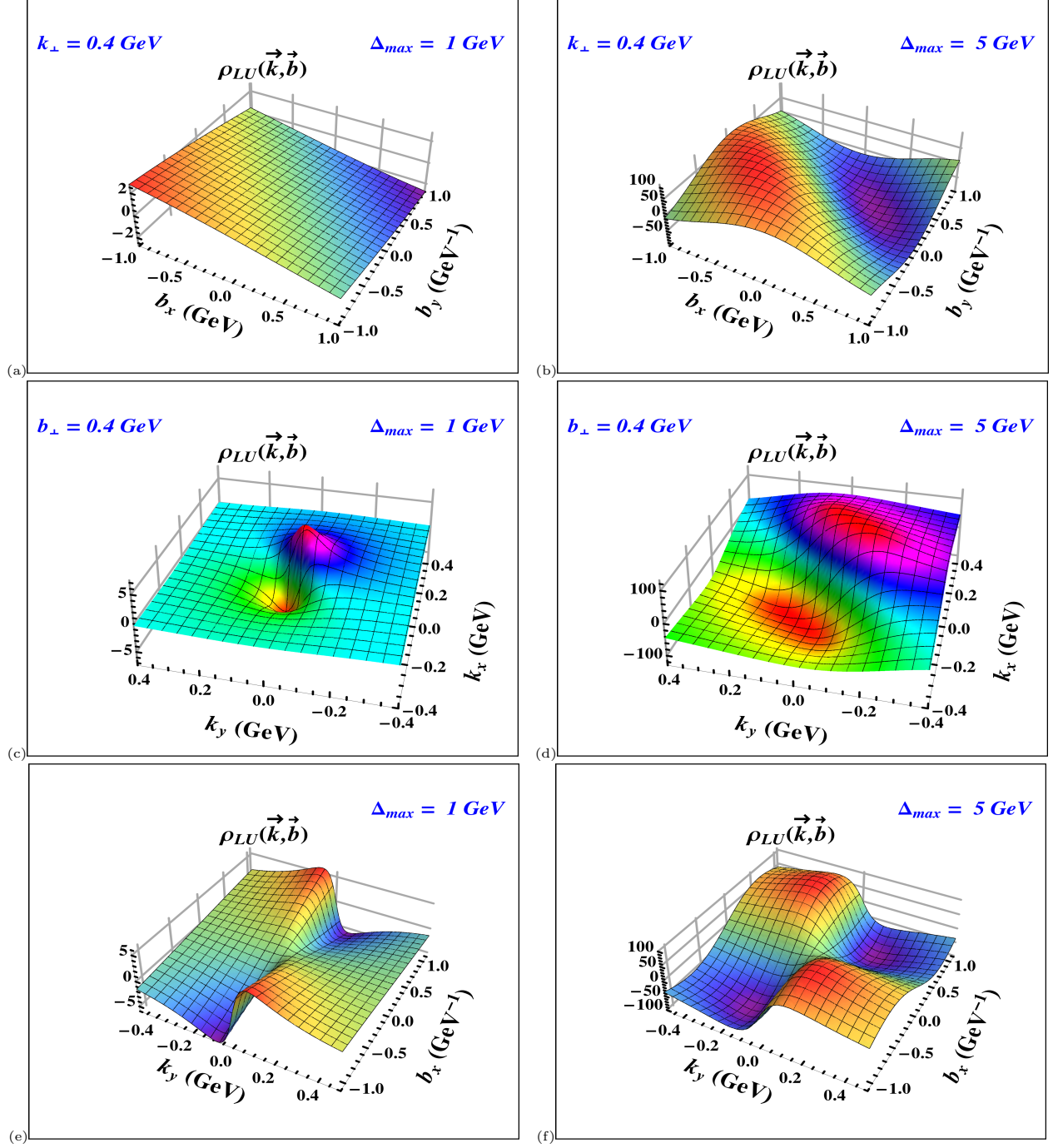


FIG. 3: (Color online) 3D plots of the Wigner distributions  $\rho_{LU}$ . Plots (a) and (b) are in  $b$  space with  $k_{\perp} = 0.4$  GeV. Plots (c) and (d) are in  $k$  space with  $b_{\perp} = 0.4$  GeV $^{-1}$ . Plots (e) and (f) are in mixed space where  $k_x$  and  $b_y$  are integrated. All the plots on the left panel (a,c,e) are for  $\Delta_{max} = 1.0$  GeV. Plots on the right panel (b,d,f) are for  $\Delta_{max} = 5.0$  GeV. For all the plots we kept  $m = 0.33$  GeV, integrated out the  $x$  variable and we took  $\vec{k}_{\perp} = k\hat{j}$  and  $\vec{b}_{\perp} = b\hat{j}$ .

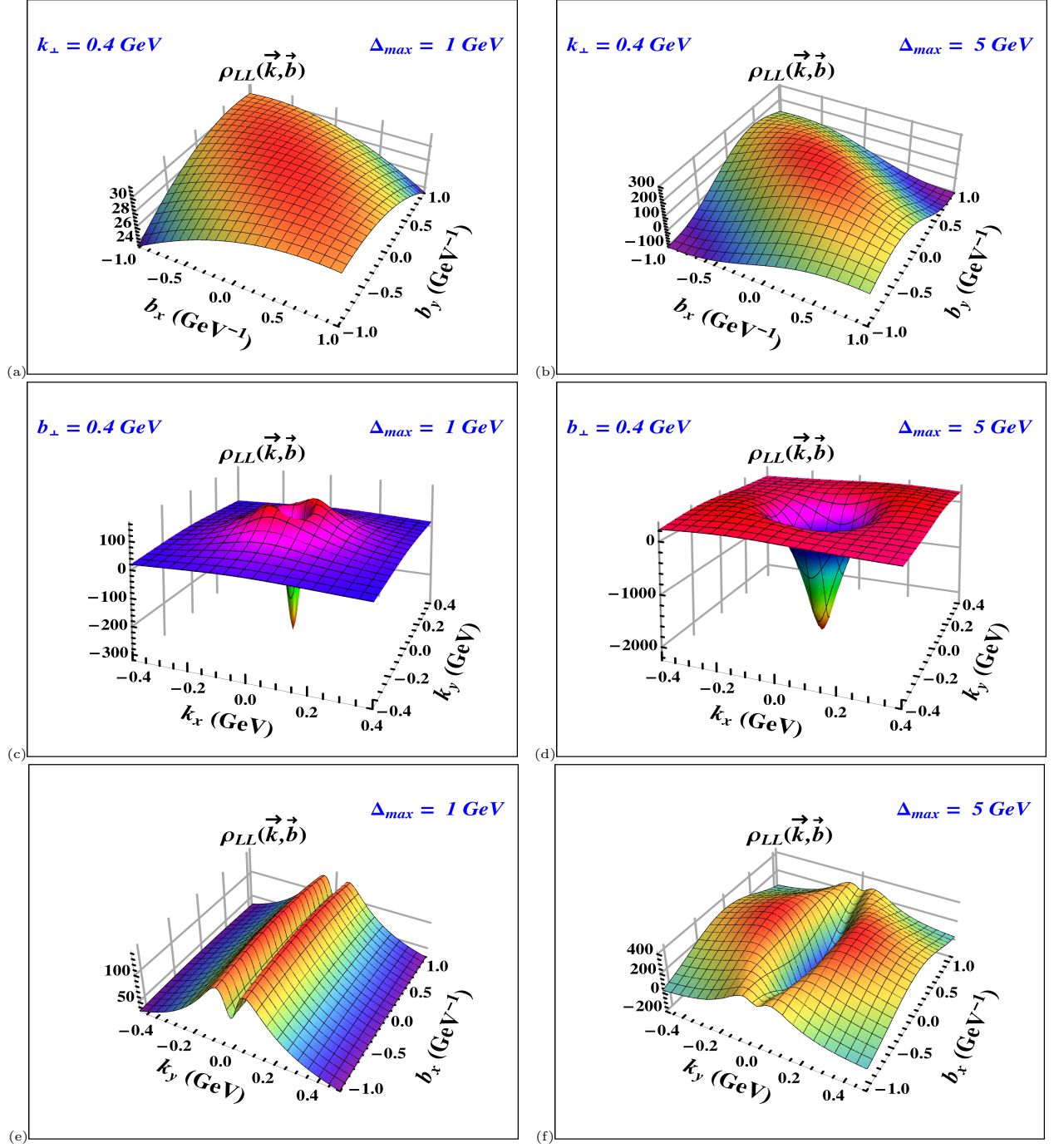


FIG. 4: (Color online) 3D plots of the Wigner distributions  $\rho_{LL}$ . Plots (a) and (b) are in  $b$  space with  $k_{\perp} = 0.4 \text{ GeV}$ . Plots (c) and (d) are in  $k$  space with  $b_{\perp} = 0.4 \text{ GeV}^{-1}$ . Plots (e) and (f) are in mixed space where  $k_x$  and  $b_y$  are integrated. All the plots on the left panel (a,c,e) are for  $\Delta_{max} = 1.0 \text{ GeV}$ . Plots on the right panel (b,d,f) are for  $\Delta_{max} = 5.0 \text{ GeV}$ . For all the plots we kept  $m = 0.33 \text{ GeV}$ , integrated out the  $x$  variable and we took  $\vec{k}_{\perp} = k_{\hat{j}}$  and  $\vec{b}_{\perp} = b_{\hat{j}}$ .

$$W_{\lambda,\lambda'}^{[\gamma^+\gamma_5]} = \frac{\bar{u}(p', \lambda')}{2M} \left[ \frac{-i\epsilon_{\perp}^{ij} k_{i\perp} \Delta_{j\perp}}{M^2} G_{1,1} - \frac{i\sigma^{i+} \gamma_5 k_{i\perp}}{P^+} G_{1,2} - \frac{i\sigma^{i+} \gamma_5 \Delta_{i\perp}}{P^+} G_{1,3} + i\sigma^{+-} \gamma_5 G_{1,4} \right] u(p, \lambda).$$

Using the above two equations and Eq.(1) we calculate the GTMDs for the dressed quark model at twist two. We have used the Bjorken and Drell convention for gamma matrices. Using the two-particle LFWFs we obtain the final expression for the GTMDS as follows :

$$F_{11} = -\frac{N \left[ 4k_{\perp}^2 (1+x^2) + (x-1)^2 (4m^2(x-1)^2 - (1+x^2)\Delta_{\perp}^2) \right]}{D(q_{\perp})D(q'_{\perp})2x^2(x-1)^3}; \quad (15)$$

$$F_{12} = \frac{2Nm^2\Delta_{\perp}^2}{D(q_{\perp})D(q'_{\perp})x(k_y\Delta_x - k_x\Delta_y)}; \quad (16)$$

$$F_{13} = \frac{N}{D(q_{\perp})D(q'_{\perp})4x(k_y\Delta_x - k_x\Delta_y)} \left[ 8m^2(k_{\perp}\Delta_{\perp}) - \frac{(k_y\Delta_x - k_x\Delta_y)(4k_{\perp}^2(1+x^2) + (x-1)^2(4m^2(x-1)^2 - (1+x^2)\Delta_{\perp}^2))}{x(x-1)^3} \right]; \quad (17)$$

$$F_{14} = \frac{2Nm^2(1+x)}{D(q_{\perp})D(q'_{\perp})x^2(1-x)}. \quad (18)$$

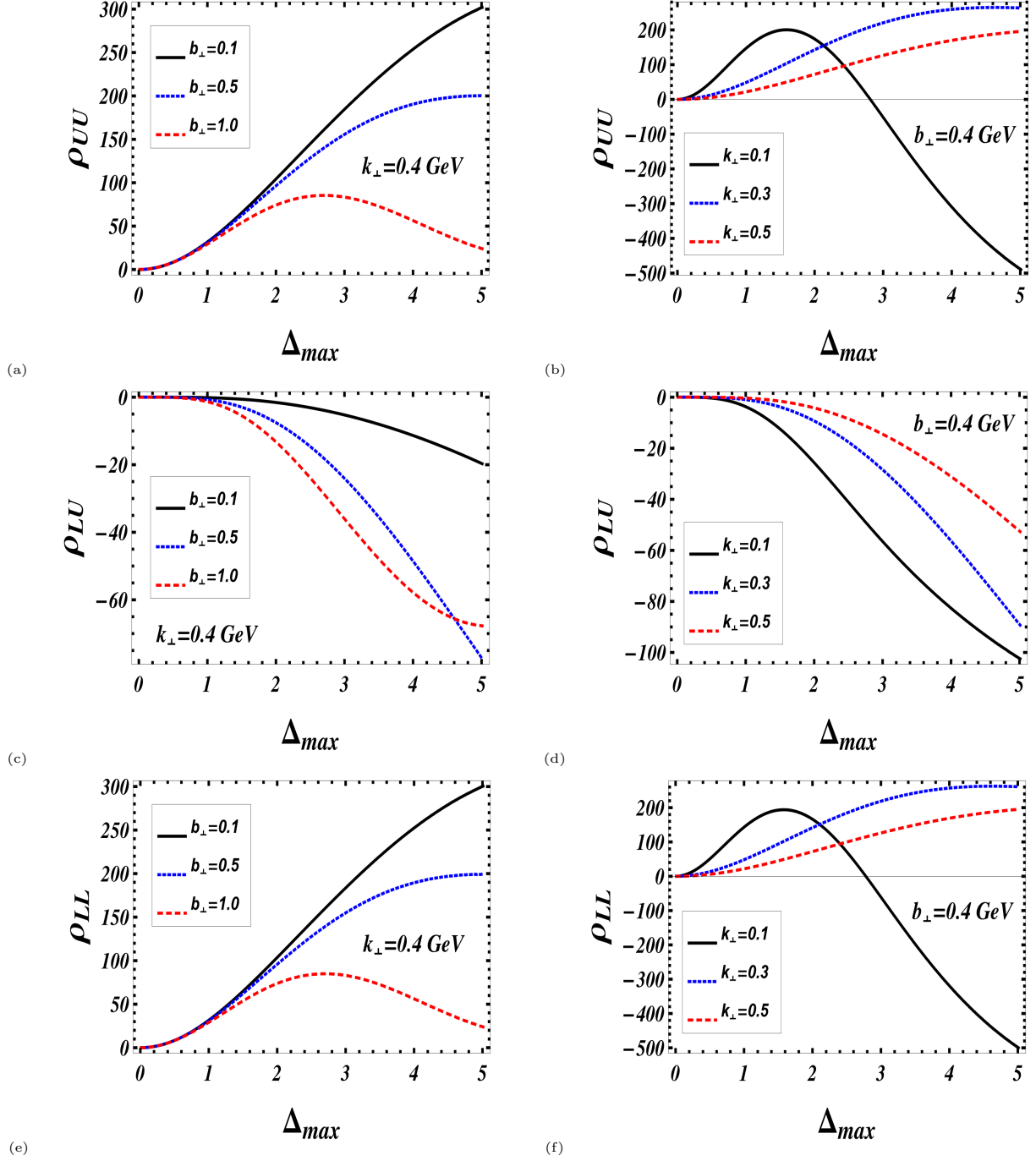


FIG. 5: (Color online) Plots of the Wigner distributions vs  $\Delta_{max}(\text{GeV})$  for fixed values of  $b_{\perp}$  and  $k_{\perp}$  at  $m = 0.33 \text{ GeV}$ . All the plots on the left (a,c,e) are for three fixed values of  $b_{\perp}$  (0.1,0.5,1.0) in  $\text{GeV}^{-1}$  where  $k_{\perp} = 0.4 \text{ GeV}$ . Plots on the right (b,d,f) are for three fixed values of  $k_{\perp}$  (0.1,0.3,0.5) in  $\text{GeV}$  where  $b_{\perp} = 0.4 \text{ GeV}^{-1}$ . For all plots we took  $\vec{k}_{\perp} = k\hat{j}$  and  $\vec{b}_{\perp} = b\hat{j}$ .



$$G_{11} = -\frac{2Nm^2(1+x)}{D(q_\perp)D(q'_\perp)x^2(x-1)}; \quad (19)$$

$$G_{12} = \frac{-N}{D(q_\perp)D(q'_\perp)x(x-1)} \left[ 4m^2 \frac{k_\perp \cdot \Delta_\perp}{(k_y \Delta_x - k_x \Delta_y)} - \frac{(1+x)\Delta_\perp^2}{x} \right]; \quad (20)$$

$$G_{13} = \frac{N \left[ (1+x) \left( \Delta_y^2 - \Delta_x^2 + \Delta_x \Delta_y (k_y^2 - k_x^2) \right) + 4xm^2 k_\perp^2 \right]}{D(q_\perp)D(q'_\perp)x^2(x-1)(k_y \Delta_x - k_x \Delta_y)}; \quad (21)$$

$$G_{14} = \frac{N \left[ -4k_\perp^2(1+x^2) + (x-1)^2 \left( 4m^2(x-1)^2 - (1+x^2)\Delta_\perp^2 \right) \right]}{D(q_\perp)D(q'_\perp)2x^2(x-1)^3}; \quad (22)$$

where  $N = \frac{g^2}{2(2\pi)^3}$  is the normalization constant.

The kinetic quark orbital angular momentum (OAM) is given in terms of the GPDs [12] as:

$$L_z^q = \frac{1}{2} \int dx \{ x [H^q(x, 0, 0) + E^q(x, 0, 0)] - \tilde{H}^q(x, 0, 0) \}.$$

The GPDs in the above equation are defined at  $\xi = 0$  or when the momentum transfer is purely in the transverse direction. GPDs in the model we consider have been already calculated in [13],[14],[15],[16]. The kinetic OAM is related to the GTMDs [4] by the following relations :

$$H(x, 0, t) = \int d^2 k_\perp F_{11}; \quad (23)$$

$$E(x, 0, t) = \int d^2 k_\perp \left[ -F_{11} + 2 \left( \frac{k_\perp \cdot \Delta_\perp}{\Delta_\perp^2} F_{12} + F_{13} \right) \right]; \quad (24)$$

$$\tilde{H}(x, 0, t) = \int d^2 k_\perp G_{14}. \quad (25)$$

Using the GTMDs calculated we have the following final expression for the kinetic orbital angular momentum of quarks in the dressed quark model:

$$L_z^q = \frac{N}{2} \int dx \left\{ -f(x)I_1 + 4m^2(1-x)^2I_2 \right\}; \quad (26)$$

where,

$$\begin{aligned} I_1 &= \int \frac{d^2k_\perp}{m^2(1-x)^2 + (k_\perp)^2} = \pi \log \left[ \frac{Q^2 + m^2(1-x)^2}{\mu^2 + m^2(1-x)^2} \right]; \\ I_2 &= \int \frac{d^2k_\perp}{\left(m^2(1-x)^2 + (k_\perp)^2\right)^2} = \frac{\pi}{(m^2(1-x)^2)}; \\ f(x) &= 2(1+x^2). \end{aligned}$$

Here  $Q$  and  $\mu$  are the upper and lower limits of the integration respectively,  $\mu$  can be safely taken to be zero provided the quark mass is non-zero. In fact, we have taken  $\mu$  to be zero.

Unlike the GTMDs  $F_{1,1-3}$ ,  $F_{1,4}$  is not reducible to any GPDs or transverse-momentum dependent parton distributions (TMDs) in any limit. It is appearing purely at the level of the GTMDs and is related to the canonical OAM as shown in [5, 17]:

$$l_z^q = - \int dx d^2k_\perp \frac{k_\perp^2}{m^2} F_{14}. \quad (27)$$

We again give the final expression for the canonical quark OAM in the dressed quark model.

$$l_z^q = -2N \int dx (1-x^2) \left[ I_1 - m^2(x-1)^2 I_2 \right]. \quad (28)$$

The above expression is in agreement with [10], where the authors have calculated the quark canonical OAM using the same model neglecting the quark mass. Our results are also in agreement with [18].

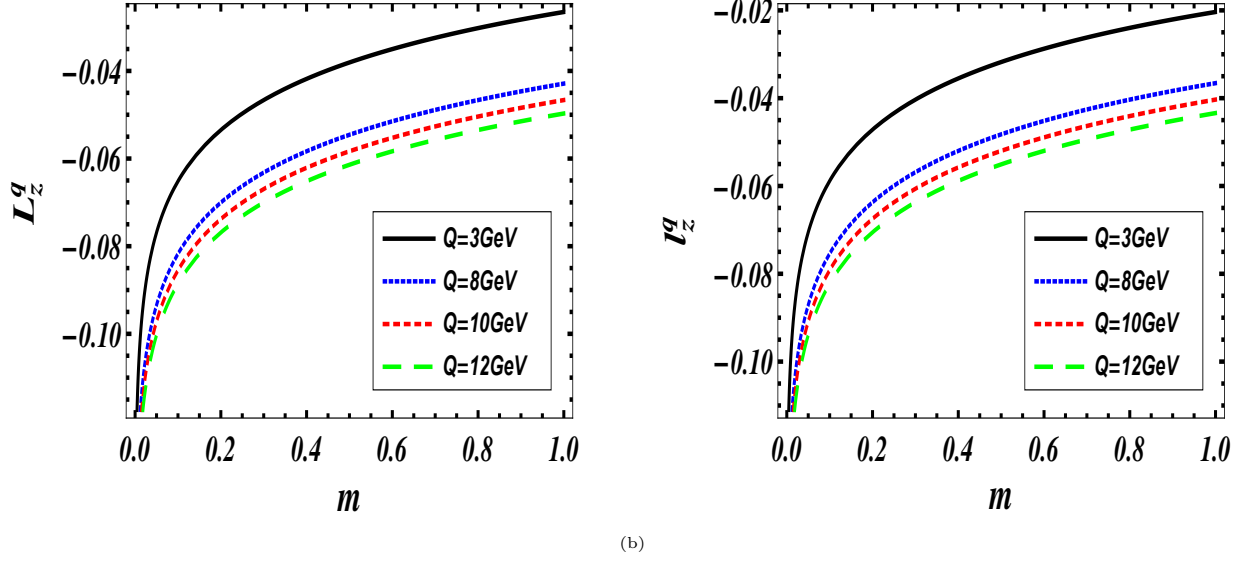


FIG. 6: (Color online) Plots of OAM (a)  $L_z^q$  and (b)  $l_z^q$  vs  $m$  (GeV) for different values of  $Q$  (GeV).

#### IV. NUMERICAL RESULTS

In all plots, we have integrated over  $x$ . In Fig. 1 we show the dependence of the Wigner distributions on the quark mass. We took the mass of the dressed quark to be the same as the bare quark. Here we have plotted the Wigner distributions versus the mass for fixed values of  $b_\perp$  in  $\text{GeV}^{-1}$  and  $k_\perp$  in  $\text{GeV}$ . Ideally the upper limit of the  $\Delta_\perp$  integration should be infinity. However we have imposed an upper cutoff  $\Delta_{max}$  in the numerical integration. In Fig. 1 we have taken  $\Delta_{max} = 1.0$  GeV. Here  $\vec{b}_\perp = b_\perp \hat{j}$  and  $\vec{k}_\perp = k_\perp \hat{j}$ . For  $\rho_{UU}$  in Fig. 1 (a) we have plotted the mass dependence for three different values of  $b_\perp$  which are 0.1, 0.5 and 1.0  $\text{GeV}^{-1}$  keeping  $k_\perp = 0.4$  GeV and we see that the value decreases with increasing mass. This is because the mass term in the denominator of Eq.(11) coming from the  $D(k)$  function is dominant over the other term. For larger  $b_\perp$  values the distribution has smaller values as seen from the plot. In Fig. 1 (b) we have plotted the mass dependence for three different values of  $k_\perp$  which are 0.1, 0.3 and 0.5  $\text{GeV}$  keeping  $b_\perp = 0.4$   $\text{GeV}^{-1}$ . Again we see the same behavior as in Fig. 1 (a), in the lower mass range  $\rho_{UU}$  increases sharply for smaller  $k_\perp$ . In fig. 1 (c) and fig. 1 (d) we have plotted the mass dependence for  $\rho_{LU}$  with the same settings as for  $\rho_{UU}$ . Since we choose  $\vec{k}_\perp = k_\perp \hat{j}$  and because of the  $k_x \Delta_y - k_y \Delta_x$  we observe that the distribution has negative values but we do observe the same behavior as seen previously. Lastly in Fig. 1 (e) and Fig.

1 (f) we show the results for  $\rho_{LL}$ . Since  $\rho_{UU}$  and  $\rho_{LL}$  only differ by a sign in their mass term as seen in Eqs.(11-13), the results are nearly identical, as the mass term gives sub-dominant contribution. In all the plots of 1 we observe that at higher mass range the distributions are nearly independent of  $b_{\perp}$  and  $k_{\perp}$  values.

In Fig. 2 we show the 3D plots for the Wigner distribution  $\rho_{UU}$ . In the numerical calculation for Eq.11 we have upper cut-off's  $\Delta_x^{max}$  and  $\Delta_y^{max}$  for the  $\Delta_{\perp}$  integration. In all plots we have taken  $m = 0.33$  GeV. In Figs. (2a) and (2b) we have plotted  $\rho_{UU}$  in  $b$  space with  $k_{\perp} = 0.4$  GeV such that  $\vec{k}_{\perp} = k\hat{j}$  for  $\Delta_{\perp}^{max} = 1.0$  GeV and  $\Delta_{\perp}^{max} = 5.0$  GeV respectively. We see that the plot has a peak centered at  $b_x = b_y = 0$  decreasing in the outer regions of the  $b$  space. In [5] the authors have shown that the contour plots show asymmetry associated with the orbital angular momentum and the asymmetry favored the  $b \perp k$  direction to  $b \parallel k$ . This can be understood from semi-classical arguments in a model with confinement. As no confining potential is present in the perturbative model we consider here, the behavior is expected to be different. In our case we observe the asymmetry but there is no particular favored direction for this asymmetry. In Figs. (2c) and (2d) we have plots in the  $k$  space where  $b_{\perp} = 0.4$  GeV such that  $\vec{b}_{\perp} = b\hat{j}$  for  $\Delta_{\perp}^{max} = 1.0$  GeV and  $\Delta_{\perp}^{max} = 5.0$  GeV respectively. The behavior in the  $k$  space is similar to that in the  $b$  space but the peaks have negative values. In Fig. (2e) and (2f) we show the plots in the mixed space. As discussed earlier, Wigner distributions do not have probability interpretation due to uncertainty principle in quantum mechanics. However in the distributions  $\rho_{UU}(k_y, b_x)$  we have integrated out the  $k_x$  and  $b_y$  dependence giving us the probability densities correlating  $k_y$  and  $b_x$ , this correlation is not restricted by uncertainty principle. Unlike in [5] we observe a minima at  $b_x = 0$  and  $k_y = 0$ . In fact the minima is observed for all  $b_x$  values for  $k_y = 0$ . As  $\Delta_{max}$  increases the minima gets deeper. The plots show that the probability of finding a quark with fixed  $k_y$  and  $b_x$  first increases away from  $k_y = 0$  and then decreases.

In Fig. 3 we show the 3D plots for the Wigner distribution  $\rho_{LU}$ . This is the distortion of the Wigner distribution of unpolarized quarks due to the longitudinal polarization of the nucleon. In fig. (3a) and (3b) we have plotted  $\rho_{LU}$  in  $b$  space with  $k_{\perp} = 0.4$  GeV such that  $\vec{k}_{\perp} = k\hat{j}$  for  $\Delta_{\perp}^{max} = 1.0$  GeV and  $\Delta_{\perp}^{max} = 5.0$  GeV respectively. Like in [5] we observe a dipole structure in these plots and the dipole magnitude increases with increase in  $\Delta_{max}$ . In Fig. (3c) and

(3d) we have plots in the  $k$  space where  $b_\perp = 0.4$  GeV such that  $\vec{b}_\perp = b\hat{j}$  for  $\Delta_\perp^{max} = 1.0\text{GeV}$  and  $\Delta_\perp^{max} = 5.0$  GeV respectively. Again we observe a dipole structure but the orientation is rotated in the  $k$  space when compared to the  $b$  space plots of Fig. (3a) and Fig. (3b). As before the dipole magnitude increases with increase in  $\Delta_{max}$ . In fig. (3e) and (3f) we show the plots in the mixed space. We observe the quadrupole structure in the mixed space like in [5] and the peaks increase in magnitude with increasing  $\Delta_\perp^{max}$ .

In Fig 4 we show the 3D plots for the Wigner distribution  $\rho_{LL}$ . The behavior is similar to that of Fig 2 since the Wigner distribution functions  $\rho_{UU}$  and  $\rho_{LL}$  only differ by the sign of the mass term in the numerator. In Fig. 5 we study the  $\Delta_\perp^{max}$  dependence of the Wigner distributions. As stated before, in the ideal definition of the Fourier transform the upper limit of the  $\Delta_\perp$  integration should be infinite. In our calculation we took a finite upper limit. In Fig. (5a) we show the dependence of  $\rho_{UU}$  on  $\Delta_\perp^{max}$  for different fixed values of  $b_\perp$  at  $k_\perp = 0.4$  GeV. For all these plots we have  $\vec{b}_\perp = b\hat{j}$  and  $\vec{k}_\perp = k\hat{j}$  and  $m = 0.33$  GeV. We observe that as  $\Delta_\perp^{max}$  increases the curve for  $b_\perp = 0.1 \text{ GeV}^{-1}$  increases faster followed by  $b_\perp = 0.5 \text{ GeV}^{-1}$  and then  $b_\perp = 1.0 \text{ GeV}^{-1}$  and the distribution is independent of  $b_\perp$  values for small  $\Delta_\perp^{max}$ . In Fig. (5b) we show  $\rho_{UU}$  vs  $\Delta_\perp^{max}$  for different fixed values of  $k_\perp$  at  $b_\perp = 0.4\text{GeV}^{-1}$ . We see a similar behavior as in Fig. (5a). In Fig. (5c) we show  $\rho_{LU}$  vs  $\Delta_\perp^{max}$  for different fixed values of  $b_\perp$  at  $k_\perp = 0.4$  GeV and in Fig. (5d) we show it for different fixed values of  $k_\perp$  at  $b_\perp = 0.4 \text{ GeV}^{-1}$ . For small  $\Delta_\perp^{max}$  values we observe a similar behavior as  $\rho_{UU}$ . Because of the term  $k_x\Delta_y - k_y\Delta_x$  and since  $\vec{k}_\perp = k\hat{j}$  we observe negative values for  $\rho_{LU}$ . In Fig. (5e) and (5f) we show  $\rho_{LL}$  vs  $\Delta_\perp^{max}$  for different fixed values of  $b_\perp$  and  $k_\perp$  and the behavior is similar to  $\rho_{UU}$ .

In Fig.6 we have shown the orbital angular momentum of quarks as a function of the mass. Fig (6a) is for  $L_z^q$  and (6b) for  $l_z^q$ . Both the plots are shown for different  $Q$  values in GeV where  $Q$  is the upper limit in the momentum integration. We see similar qualitative behavior of  $L_z^q$  and  $l_z^q$  where both are giving negative values for the chosen domain of mass and also both the OAM increases with increasing mass. However the magnitude of the two OAM differs in our model, unlike the case in [5], where the same had been calculated in several models without any gluonic degrees of freedom and the total quark contribution to the OAM were equal for

both cases. Thus our simple model explicitly shows the contribution of the gluonic degrees of freedom to the OAM. In fact in [10] it was shown that in the model considered here, after the inclusion of the single particle sector of the Fock space (which contributes at  $x = 1$ ), the gluon intrinsic helicity contribution to the helicity sum rule cancels the contribution from the quark and gluon OAM and the helicity sum rule is satisfied.

## V. CONCLUSION

In this work, we calculated the Wigner distributions for a quark state dressed with a gluon using the overlap representation in terms of the LFWFs. This is a simple composite spin-1/2 system which has a gluonic degree of freedom. Although the Wigner distributions in quantum mechanics are not measurable and do not have probabilistic interpretation, after integrating out some of the variables a probabilistic interpretation is possible to obtain. We calculated the Wigner distributions both for unpolarized and longitudinally polarized target and constituent quarks and showed the correlations in transverse momentum and position space. We compared and contrasted the results with earlier calculation of Wigner distributions in light cone constituent quark model. We also calculated the kinetic quark OAM using the GPD sum rule and the canonical OAM and showed that these are different in magnitude, the difference is an effect of the gluonic degree of freedom. We also found that in the limit of zero quark mass our result for the canonical OAM agrees with that of [10]. Further work would involve calculating the Wigner distributions including transverse polarization of the target and the quark.

## VI. ACKNOWLEDGMENTS

We would like to thank C.Lorce for helpful discussion. This work is supported by the DST project SR/S2/HEP-029/2010, Govt. of India.

---

[1] E.P. Wigner, Phys.Rev. **40**, 749 (1932).

- [2] X. Ji, Phys. Rev. Lett. **91**, 062001 (2003).
- [3] A. Belitsky, X. Ji, F. Yuan; Phys.Rev. **D 69**, 074014 (2004).
- [4] S.Meissner, A.Metz,and M. Schlegel, JHEP 08 (2009) 056; S.Meissner, A.Metz, M. Schlegel and K. Goeke, JHEP 08 (2008) 038.
- [5] C. Lorce, B.Pasquini, Phys. Rev. **D84**, 014015 (2011).
- [6] A. Harindranath, Lectures given at the International School on Light-front Quantization and Non-perturbative QCD, hep-ph/9612244.
- [7] J. Ashman *et al.*, Nucl. Phys. **B328**, 1 (1989).
- [8] E. Leader, C. Lorce, arXiv:1309.4235[hep-ph]; and the references therein.
- [9] S.J.Brodsky, M.Diehl, D.S.Hwang, Nuc. Phys. **B596**, (2001) 99
- [10] A.Harindranath and R.Kundu, Phys. Rev. **D59**, 116013.
- [11] W-M. Zhang and Harindranath, Phys. Rev. **D48**, 4881 (1993).
- [12] X. Ji, Phys. Rev. Lett. **78**,610 (1997).
- [13] D. Chakrabarti, A. Mukherjee, Phys. Rev. **D 71**, 014038 (2005).
- [14] D. Chakrabarti, A. Mukherjee, Phys. Rev. **D 72**, 034013 (2005).
- [15] S. J. Brodsky, D. Chakrabarti, A. Harindranath, A. Mukherjee, J. P. Vary, Phys. Lett. **B 641**, 440 (2006).
- [16] S. J. Brodsky, D. Chakrabarti, A. Harindranath, A. Mukherjee, J. P. Vary, Phys. Rev. **D 75**, 014003 (2007).
- [17] Y. Hatta and S. Yoshida, JHEP **1210**, 080 (2012).
- [18] Hikmat BC, M. Burkardt, Few Body Syst. **52**, 389 (2012).